

Statistical Inspired Parton Distributions and the Violation of QPM Sum Rules

F. Buccella[†], I. Doršner^{†‡}, G. Miele[†], O. Pisanti[†], P. Santorelli[†], and N. Tancredi[†]

[†] *Dipartimento di Scienze Fisiche, Università di Napoli "Federico II", and INFN Sezione di Napoli, Mostra D'Oltremare Pad. 20, I-80125 Napoli, Italy*

[‡] *Prirodno-Matematički Fakultet, Univerzitet u Sarajevu, Zmaja od Bosne 32, Sarajevu, R Bosna i Hercegovina*

Abstract

A quantum statistical parametrization of parton distributions has been considered. In this framework, the exclusion Pauli principle connects the violation of the Gottfried sum rule with the Ellis and Jaffe one, and implies a defect in the Bjorken sum rule. However, in terms of standard parametrizations of the polarized distributions a good description of the data is obtained once a large gluon polarization is provided. Interestingly, in this description there is no violation of the Bjorken sum rule.

1 Statistical distributions for partons

The experimental results on deep inelastic scattering (DIS) are always an inexhaustible source for deeper insight in the nucleon structure. Among them, the violation of well established sum rules represents the relevant starting point to unveil the mechanisms which rule the parton physics. In particular, the value found by the EMC experiment [1] for the first moment of the structure function $g_1^p(x)$, $\Gamma_1^p = 0.126 \pm 0.010 \pm 0.015$, results to be smaller than the prediction based on the Ellis and Jaffe sum rule (EJ), $I_p^{EJ} = (F/2) - (D/18)$. For this reason it has generated the so-called *spin crisis*. One of the possible explanations of the EMC measurement is that it is a consequence of a negative gluon contribution [2], $-(\alpha_s/6\pi)\Delta G$, with the large positive value of ΔG balanced by a negative and large L_z . The gluonic contribution, which is related to the axial anomaly, is the same for proton and neutron and would not affect the Bjorken sum rule (Bj).

An alternative interpretation of the defect in the EJ for the proton can be found if Pauli principle plays an important role in parton distributions. Remarkably, these considerations lead to connect [3] the violation of the EJ with the observed defect in the Gottfried sum rule.

According to Feynman and Field [4], in the proton $\bar{u} < \bar{d}$ since only one valence d quark is present with respect to the two u quarks. This hypothesis would be confirmed both from the NMC measurements [5] of the Gottfried sum rule and from the CERN-NA51 experiment [6] on dilepton Drell-Yan production in pp and pn reactions. As far as the Gottfried sum rule is concerned, the NMC collaboration measures

$$\int_0^1 \frac{dx}{x} (F_2^p(x) - F_2^n(x)) = 0.235 \pm 0.026, \quad (1)$$

which, together with the Adler sum rule, implies $\bar{u} - \bar{d} = -0.15 \pm 0.04$ and $u - d = 0.85 \pm 0.04$.

A further confirmation of the Feynman and Field conjecture comes from the experimental observation that, at high x , $F_2^n(x)/F_2^p(x) \rightarrow 1/4$ and $A_1^p \rightarrow 1$. This feature, in fact, suggests that u_{val}^\uparrow is the dominating parton distribution at high x . Indeed, at $Q^2 = 0$, the axial couplings of the baryon octet are fairly described in terms of the valence quarks

$$u_{val}^\uparrow = 1 + F \quad , \quad u_{val}^\downarrow = 1 - F \quad , \quad d_{val}^\uparrow = \frac{1 + F - D}{2} \quad , \quad d_{val}^\downarrow = \frac{1 - F + D}{2} \quad . \quad (2)$$

Thus, by using the experimental values for F and D [7], one gets

$$u_{val}^\uparrow \simeq \frac{3}{2} \simeq u_{val}^\downarrow + d_{val}^\uparrow + d_{val}^\downarrow \quad . \quad (3)$$

Hence, the correlation *broader shapes* \leftrightarrow *higher abundances*, just dictated by Pauli principle, is very well verified by the experimental results. For these reasons, it is natural to assume Fermi–Dirac distributions in the variable x for the quark partons

$$p(x) = f(x) \left[\exp \left(\frac{x - \tilde{x}(p)}{\bar{x}} \right) + 1 \right]^{-1} \quad , \quad (4)$$

where \bar{x} plays the role of the temperature, $\tilde{x}(p)$ is the *thermodynamical potential* of the parton p , identified by its flavour and spin direction, and $f(x) = A x^\alpha (1-x)^\beta$ is a weight function. Analogously, for the gluons one has

$$G^{\uparrow(\downarrow)}(x) = \frac{8}{3} f(x) \left[\exp \left(\frac{x - \tilde{x}(G^{\uparrow(\downarrow)})}{\bar{x}} \right) - 1 \right]^{-1} \quad . \quad (5)$$

To recover the power behaviour of $F_2^p(x)$ at small x we add a *liquid* unpolarized component for the light quark–partons (u , d and their antiparticles), $f_L(x) = (A_L/2) x^{\alpha_L} (1-x)^{\beta_L}$, and the same x dependence, but with a different normalization for s and \bar{s} . With these distributions we try to reproduce [8] the structure functions $F_2^p(x)$, $F_2^n(x)$ [5, 9], $xF_3(x)$ [10], $g_1^p(x)$ and $g_1^d(x)$ [11, 12], at $Q^2 = 3$ and 10 $(GeV/c)^2$, considering the options with polarized or unpolarized gluons. We report

in Tables I.a and I.b the parameters and the gas abundances for partons, found with $\Delta\bar{q}_i = 0$ and with/without $\Delta G(x)$ at $Q^2 = 3$, and 10 $(GeV/c)^2$, and compare them with the results of a previous analysis. Figures 1.a–5.a and 1.b–5.b show our theoretical predictions versus the experimental data corresponding to $Q^2 = 3$ and $Q^2 = 10$ $(GeV/c)^2$ respectively, for the fits with $\Delta G = 0$ (solid line) and $\Delta G \neq 0$ (dashed line) reported in Tables I.a and I.b.

2 Standard parametrizations for the polarized distributions

In order to test in a model independent way the above two interpretations for the violation of polarized sum rules, we consider [13] a standard parametrization [14], at $Q_0^2 = 3$ $(GeV/c)^2$,

$$\begin{aligned} x\Delta u_v(x, Q_0^2) &= \eta_u A_u x^{a_u} (1-x)^{b_u} (1+\gamma_u x), \\ x\Delta d_v(x, Q_0^2) &= \eta_d A_d x^{a_d} (1-x)^{b_d} (1+\gamma_d x), \\ x\Delta G(x, Q_0^2) &= \eta_G A_G x^{a_G} (1-x)^{b_G} (1+\gamma_G x), \end{aligned} \quad (6)$$

with $A_q = A_q(a_q, b_q, \gamma_q)$ ($q = u, d, G$), in such a way that

$$\int_0^1 dx A_q x^{a_q-1} (1-x)^{b_q} (1+\gamma_q x) = 1. \quad (7)$$

We fix $\eta_d(Q_0^2) = \tilde{F} - \tilde{D} = -0.24 \pm 0.04$ and explore the two options **A** and **B**, the first one with $\eta_u(Q_0^2) = 2 \tilde{F} = 0.78 \pm 0.03$ and η_G free, the second one with η_u free and $\eta_G = 0$. Options **A** and **B** correspond to the interpretation of the defect in the EJ for proton in terms of the anomaly, assuming that the Bj is obeyed, and to the case of a smaller Δu resulting from the Pauli principle, respectively.

The parameters corresponding to the best fit of the SLAC proton and deuteron data [11] for the options **A** and **B** are given in Table II, while in Figs. 6.a and 6.b one compares the two resulting curves with SLAC data at $\langle Q^2 \rangle = 3$ $(GeV/c)^2$ with proton and deuteron targets; for the later case we take

$$g_1^d(x) = \frac{1}{2} \left(1 - \frac{3}{2} \omega_D \right) (g_1^p(x) + g_1^n(x)), \quad (8)$$

to account for the small D-wave component in the deuteron ground state, with $\omega_D = 0.058$. The evolution of the results for the two options to 2 and 10 $(GeV/c)^2$, obtained by numerically solving the Altarelli-Parisi equations, is compared with the SLAC [15] and CERN data [12] respectively in Figs. 7.a, 7.b, and 7.c.

3 Conclusions

Quantum statistical inspired distributions for quarks and gluons provide a fair description of the experimental data on deep inelastic scattering in terms of few free parameters. In this approach,

the parton distributions are given in terms of a universal *weight* function, which accounts for the parton density levels at fixed x , *thermodynamical potentials* and of a quantity which plays the role of *temperature*. Furthermore, the violations of the Gottfried and EJ sum rules result to be connected and both imply a defect in the Bj.

As far as a standard parametrization of the polarized distributions is concerned, it is worth stressing the value $\eta_u = 0.63 \pm 0.03$ for option **B**, smaller than $2\tilde{F} = 0.78 \pm 0.03$ from quark parton model, as predicted by Pauli principle. It is interesting to remark that with both options one fails to reproduce the rise of $xg_1^p(x)$ at small x , which is certainly welcome to increase the contribution to the l.h.s. of the Bj.

References

- [1] J. Ashman *et al.*, EMC Collaboration, Phys. Lett. **B206** (1988) 364; Nucl. Phys. **B328** (1989) 1.
- [2] G. Altarelli and G. G. Ross, Phys. Lett. **B212** (1988) 391; A. V. Efremov and O. V. Teryaev, Dubna Preprint **E2-88-287** (1988).
- [3] F. Buccella and J. Soffer, preprint CPT-92/P/2706; Mod. Phys. Lett. **A8** (1993) 225; Europh. Lett. **24** (1993) 165; Phys. Rev. **D48** (1993) 5416.
- [4] R.D. Field and R.P. Feynman, Phys. Rev **B15** (1977) 2590.
- [5] M. Arneodo et al. (NMC collaboration), Phys. Rev. **D50** (1994) R1.
- [6] A. Baldit et al. (NA51 collaboration), Phys. Lett. **B332** (1994) 244.
- [7] S.Y. Hsueh et al., Phys. Rev. **D38** (1988) 2056.
- [8] F. Buccella, G. Miele, and N. Tancredi, Preprint DSF-T-16/96, hep-ph/9604230.
- [9] P.Amaudruz et al., Nucl. Phys. **B371** (1992) 3; B. Foster, preprint DESY 95-158, August 1995; G. Radel (H1 collaboration), preprint DESY 95-152D, April 1995; R.G. Roberts and M.R. Whalley, J. Phys. G: Nucl. Part. Phys. **17** (1991) D1.
- [10] W.C. Leung et al. (CCFR collaboration), Phys. Lett. **B317** (1993) 655.
- [11] K. Abe *et al.*, SLAC-E143 Collaboration, Phys. Rev. Lett. **74** (1995) 346; K. Abe *et al.*, SLAC-E143 Collaboration, Phys. Rev. Lett. **75** (1995) 25.
- [12] D. Adams *et al.*, SMC Collaboration, Phys. Lett. **B329** (1994) 399; B. Adeva *et al.*, SMC Collaboration, Phys. Lett. **B302** (1993) 533; D. Adams *et al.*, SMC Collaboration, Phys. Lett. **B357** (1995) 248.

- [13] C. Bourrely, F. Buccella, O. Pisanti, P. Santorelli and J. Soffer, DSF-T-17/96, CPT-96/PE.3327, hep-ph/9604204.
- [14] T. Gehrmann and W. J. Stirling, Z. Phys. **C65** (1995) 461.
- [15] P.L. Anthony et al. (E142 collaboration), Phys. Rev. Lett. **71** (1993) 959.

Table I.a

| Param. $Q^2 = 3$ (GeV/c) ² | Previous fit ($\chi^2_{NDF} = 2.47$) | | Present fit with only $\Delta u, \Delta d \neq 0$ ($\chi^2_{NDF} = 2.33$) | | Present fit with only $\Delta u, \Delta d, \Delta G \neq 0$ ($\chi^2_{NDF} = 2.32$) | |
|---|---|------------------------|---|------------------------|---|-----------------|
| A | $2.66^{+.09}_{-.08}$ | | $2.51 \pm .07$ | | $2.54 \pm .08$ | |
| α | $-.203 \pm .013$ | | $-.231 \pm .012$ | | $-.231 \pm .011$ | |
| β | $2.34^{+.05}_{-.06}$ | | $2.21 \pm .04$ | | $2.22 \pm .04$ | |
| A_L | $.0895^{+.0107}_{-.0084}$ | | $.127^{+.016}_{-.013}$ | | $.128^{+.015}_{-.013}$ | |
| α_L | $-1.19 \pm .02$ | | $-1.18^{+.03}_{-.02}$ | | $-1.18 \pm .02$ | |
| β_L | $7.66^{+1.82}_{-1.59}$ | | $10.3^{+1.4}_{-1.3}$ | | $10.1^{+1.4}_{-1.3}$ | |
| \bar{x} | $.235 \pm .009$ | gas abund. | $.214 \pm .008$ | gas abund. | $.223 \pm .011$ | gas abund. |
| $\tilde{x}(u^\uparrow)$ | $1.00 \pm .07$ | $1.15 \pm .01$ | $1.00 \pm .02$ | $1.22 \pm .01$ | $1.00 \pm .02$ | $1.23 \pm .01$ |
| $\tilde{x}(u^\downarrow)$ | $.123 \pm .012$ | $.53 \pm .01$ | $.141 \pm .011$ | $.575 \pm .009$ | $.129^{+.014}_{-.015}$ | $.566 \pm .019$ |
| $\tilde{x}(d^\uparrow)$ | $-.068^{+.021}_{-.024}$ | $.33 \pm .03$ | $-.029^{+.019}_{-.020}$ | $.366 \pm .025$ | $-.028 \pm .020$ | $.379 \pm .030$ |
| $\tilde{x}(d^\downarrow)$ | $.200^{+.013}_{-.014}$ | $.62 \pm .01$ | $.211 \pm .011$ | $.667 \pm .006$ | $.196^{+.015}_{-.016}$ | $.651 \pm .017$ |
| $\tilde{x}(\bar{u}^\uparrow)$ | $-.886 \pm .266$ | $.015^{+.034}_{-.009}$ | $-.522^{+.049}_{-.061}$ | $.054^{+.021}_{-.022}$ | $-.559^{+.057}_{-.075}$ | $.052 \pm .022$ |
| $\tilde{x}(\bar{u}^\downarrow)$ | " | " | " | " | " | " |
| $\tilde{x}(\bar{d}^\uparrow)$ | $-.460^{+.047}_{-.064}$ | $.08^{+.03}_{-.02}$ | $-.339^{+.032}_{-.040}$ | $.12 \pm .03$ | $-.366^{+.037}_{-.049}$ | $.12 \pm .03$ |
| $\tilde{x}(\bar{d}^\downarrow)$ | " | " | " | " | " | " |
| $\tilde{x}(G^\uparrow)$ | $-.067$ | 3.16 | $-.067^{+.008}_{-.009}$ | $2.93 \pm .40$ | $-.069 \pm .09$ | $3.04 \pm .55$ |
| $\tilde{x}(G^\downarrow)$ | " | " | " | " | $-.085^{+.015}_{-.019}$ | $2.56 \pm .61$ |

The parameters and the gas abundances for partons, found with $\Delta \bar{q}_i = 0$ and with/without $\Delta G(x)$ at $Q^2 = 3$ (GeV/c)² are reported and compared with the results of a previous analysis. Note that, no antiquarks or strange quark polarization is assumed.

Table I.b

| Parameters $Q^2 = 10$ (GeV/c) ² | Present fit with only $\Delta u, \Delta d \neq 0$ ($\chi^2_{NDF} = 0.98$) | | Present fit with only $\Delta u, \Delta d, \Delta G \neq 0$ ($\chi^2_{NDF} = 0.95$) | |
|--|---|--------------------|---|--------------------|
| A | 2.00 | $^{+.15}_{-.13}$ | 1.99 | $^{+.19}_{-.14}$ |
| α | -.363 | $^{+.042}_{-.035}$ | -.375 | $^{+.046}_{-.035}$ |
| β | 2.29 ± .04 | | 2.28 | $^{+.05}_{-.04}$ |
| A_L | .108 | $^{+.018}_{-.014}$ | .109 | $^{+.022}_{-.016}$ |
| α_L | -1.29 ± .02 | | -1.28 | $^{+.03}_{-.02}$ |
| β_L | 10.1 | $^{+3.7}_{-3.5}$ | 11.1 | $^{+4.7}_{-4.3}$ |
| \bar{x} | .238 | $^{+.009}_{-.007}$ | gas abund. | |
| $\tilde{x}(u^\uparrow)$ | 1.00 ± .01 | 1.32 | $^{+.05}_{-.06}$ | 1.00 ± .01 |
| $\tilde{x}(u^\downarrow)$ | .104 | $^{+.038}_{-.043}$ | .617 | $^{+.012}_{-.030}$ |
| $\tilde{x}(d^\uparrow)$ | -.114 | $^{+.050}_{-.070}$ | .36 | $^{+.04}_{-.06}$ |
| $\tilde{x}(d^\downarrow)$ | .171 | $^{+.022}_{-.027}$ | .704 | $^{+.014}_{-.003}$ |
| $\tilde{x}(\bar{u}^\uparrow)$ | -.69 | $^{+.13}_{-.20}$ | .044 | $^{+.067}_{-.049}$ |
| $\tilde{x}(\bar{u}^\downarrow)$ | " | " | " | " |
| $\tilde{x}(\bar{d}^\uparrow)$ | -.412 ± .12 | .130 | $^{+.001}_{-.025}$ | -.40 ± .10 |
| $\tilde{x}(\bar{d}^\downarrow)$ | " | " | " | " |
| $\tilde{x}(G^\uparrow)$ | -.086 ± 0.003 | 3.519 | $^{+.001}_{-.025}$ | -.076 |
| $\tilde{x}(G^\downarrow)$ | " | " | " | " |

The same quantities of Table I.a are shown for $Q^2 = 10$ (GeV/c)².

Table II

| | $a_u = a_d$ | b_u | $\gamma_u = \gamma_d$ | b_d | a_G | b_G | γ_G |
|----------|--------------------------------|---------------------------|------------------------------|-----------------------|-------|-------------------|------------------|
| A | $0.52 \pm 0.09^{(*)}$ | $1.7 \pm 0.3^{(*)}$ | $2.8^{+3.7}_{-1.9}^{(*)}$ | $3.0 \pm 0.5^{(*)}$ | 1 | $20 \pm 11^{(*)}$ | $0 \pm 14^{(*)}$ |
| | $\eta_u = 0.78 \pm 0.03$ | $\eta_d = -0.24 \pm 0.02$ | $\eta_G = 1.1 \pm 0.5^{(*)}$ | $\chi^2_{NDF} = 1.04$ | | | |
| B | $1.0 \pm 0.1^{(*)}$ | $1.8^{+0.5}_{-0.2}^{(*)}$ | $0.0 \pm 2.7^{(*)}$ | $4.1 \pm 1.1^{(*)}$ | - | - | - |
| | $\eta_u = 0.63 \pm 0.03^{(*)}$ | $\eta_d = -0.24 \pm 0.02$ | $\eta_G = 0$ | $\chi^2_{NDF} = 1.08$ | | | |

The results of the options **A** and **B** (see text) for the values of the parameters of the fits at $Q^2 = 3$ (GeV/c)². The free parameters are marked with an asterisk.

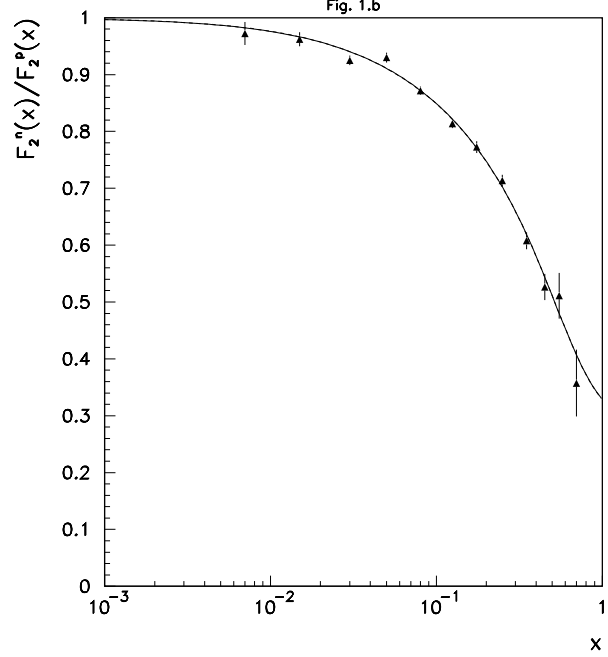
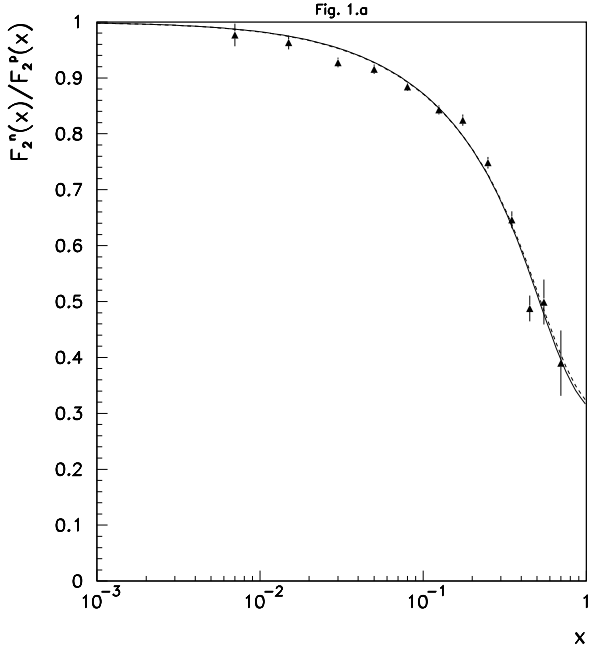


Figure 1.a The prediction for $F_2^n(x)/F_2^p(x)$ at $Q^2 = 3 \text{ (GeV/c)}^2$ is plotted and compared with the experimental data [9], the solid line and the dashed line corresponds to the fit with $\Delta G = 0$ and $\Delta G \neq 0$ of Table I.a, respectively. This notation is valid for all Figures 1.a-5.a.

Figure 1.b The same quantity of Figure 1.a is plotted for $Q^2 = 10 \text{ (GeV/c)}^2$, the solid line and the dashed line corresponds to the fit with $\Delta G = 0$ and $\Delta G \neq 0$ of Table I.b, respectively. This notation is valid for all Figures 1.b-5.b.

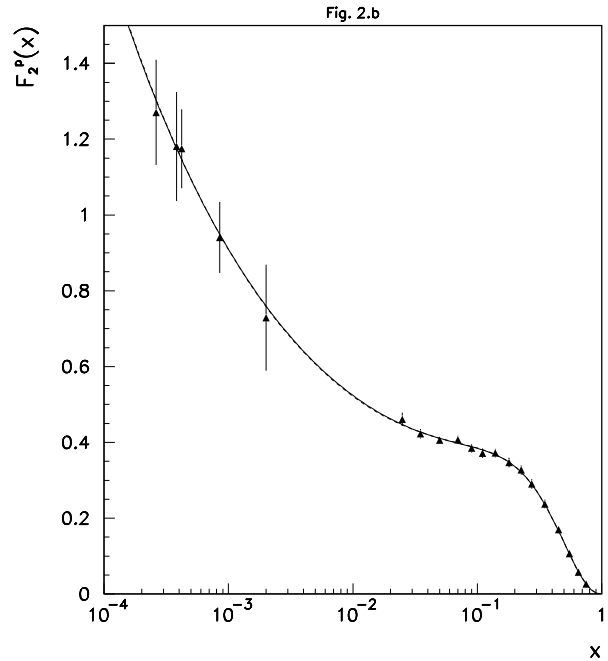
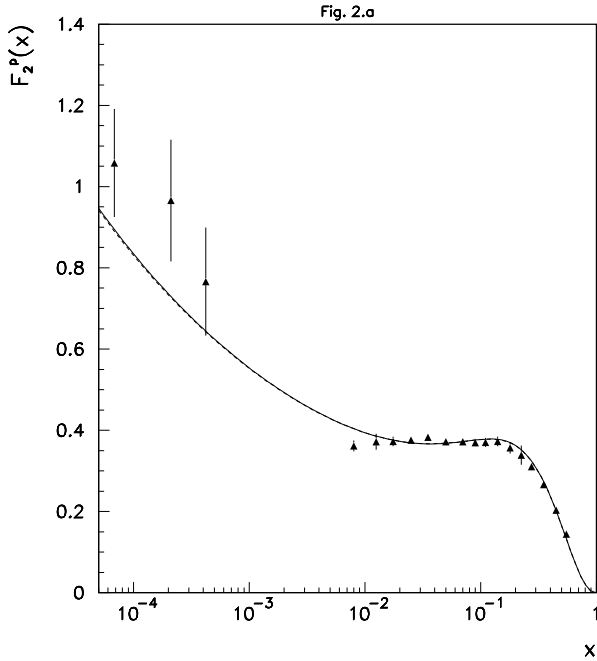


Figure 2.a The prediction for $F_2^p(x)$ at $Q^2 = 3 \text{ (GeV/c)}^2$ is plotted and compared with the experimental data [9].

Figure 2.b The same quantity of Figure 2.a is plotted for $Q^2 = 10 \text{ (GeV/c)}^2$.

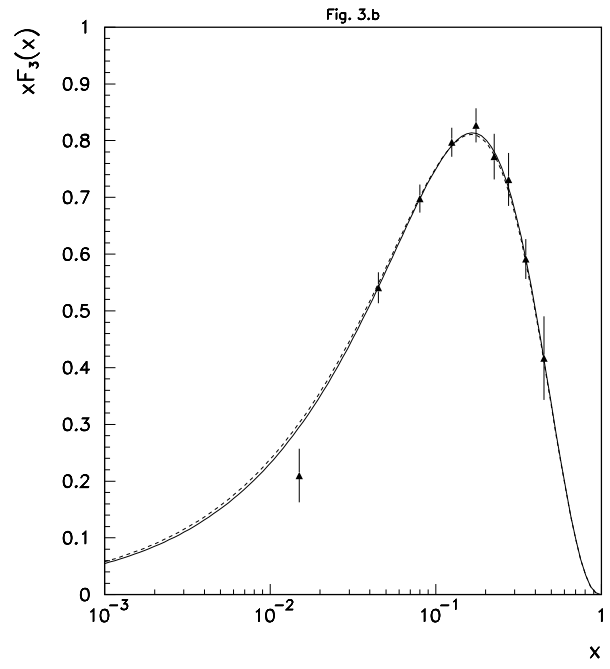
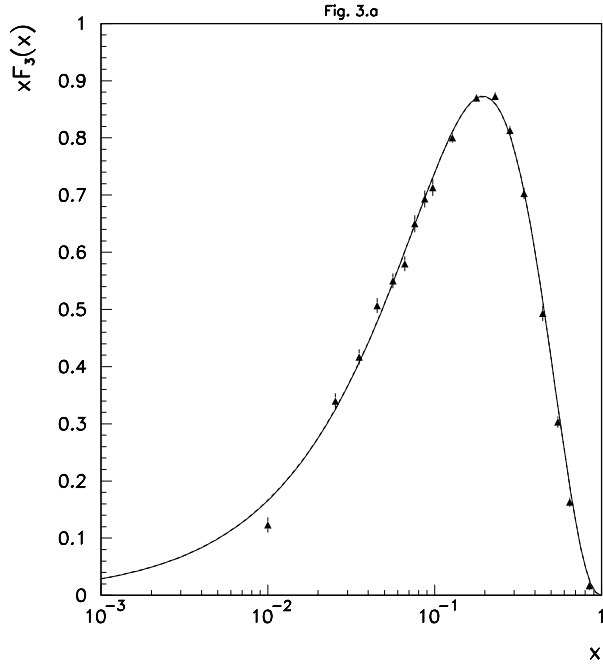


Figure 3.a $xF_3(x)$ is plotted for $Q^2 = 3 \text{ (GeV/c)}^2$ and the experimental values are taken from [10].

Figure 3.b $xF_3(x)$ is plotted for $Q^2 = 10 \text{ (GeV/c)}^2$ and the experimental values are taken from [10].

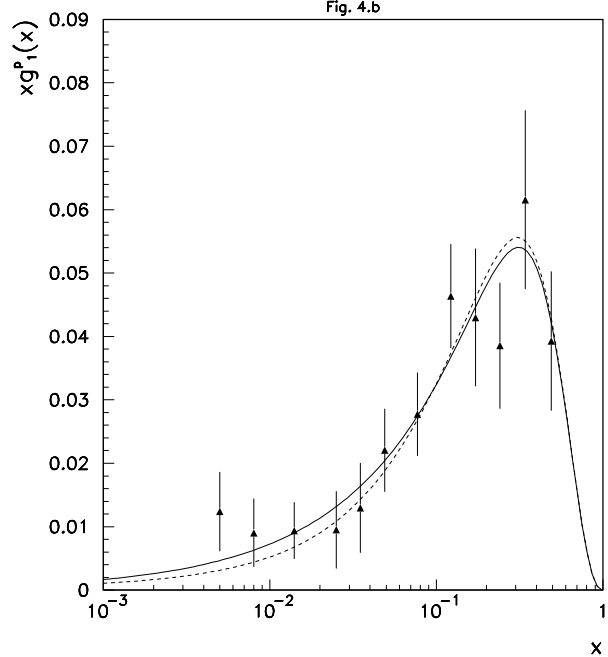
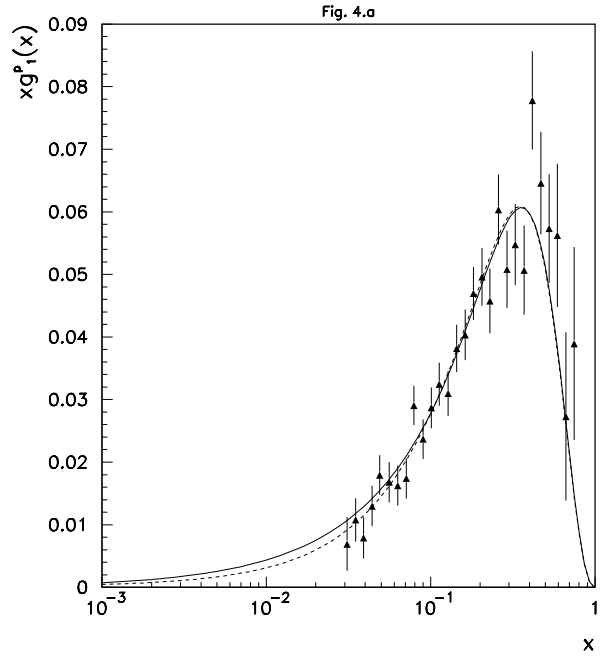


Figure 4.a $xg_1^p(x)$ at $Q^2 = 3 \text{ (GeV/c)}^2$ is plotted and compared with the data [11].

Figure 4.b The same quantity of Figure 4.a corresponding to $Q^2 = 10 \text{ (GeV/c)}^2$ is plotted versus the experimental data [12].

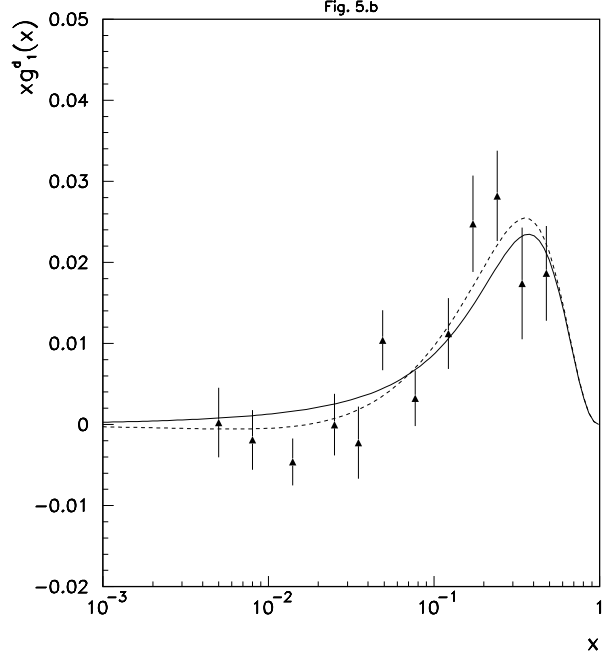
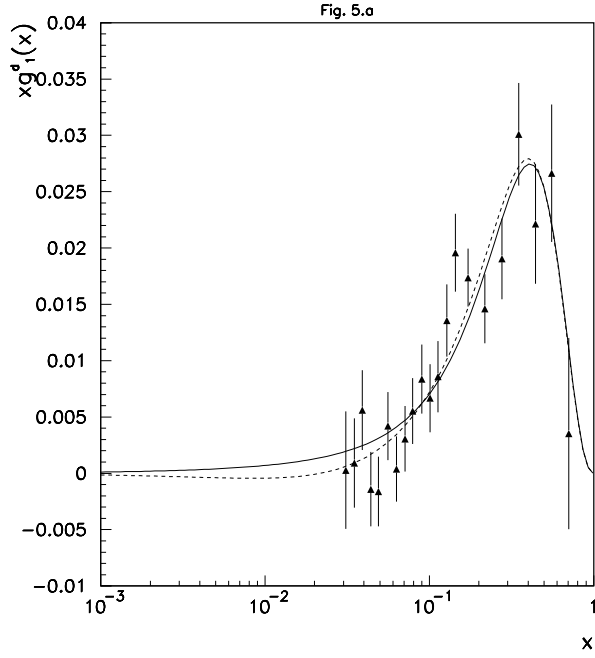


Figure 5.a $xg_1^d(x)$ at $Q^2 = 3 \text{ (GeV/c)}^2$ is plotted and compared with the data [11].

Figure 5.b The same quantity of Figure 5.a corresponding to $Q^2 = 10 \text{ (GeV/c)}^2$ is plotted versus the experimental data [12].

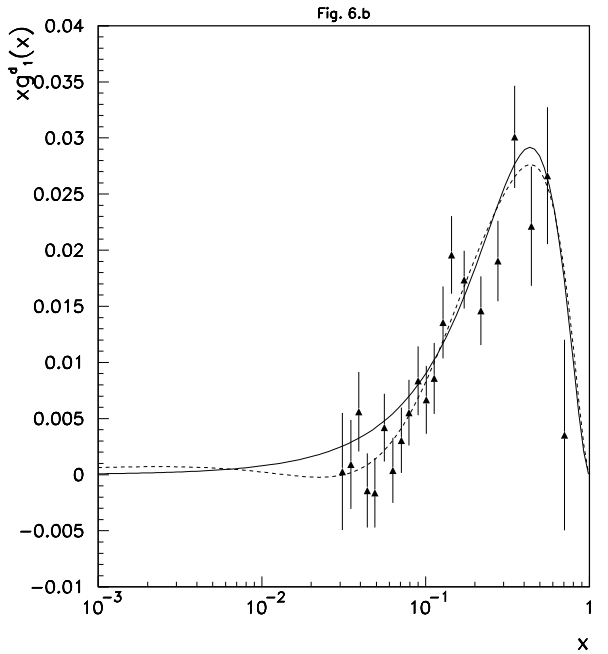
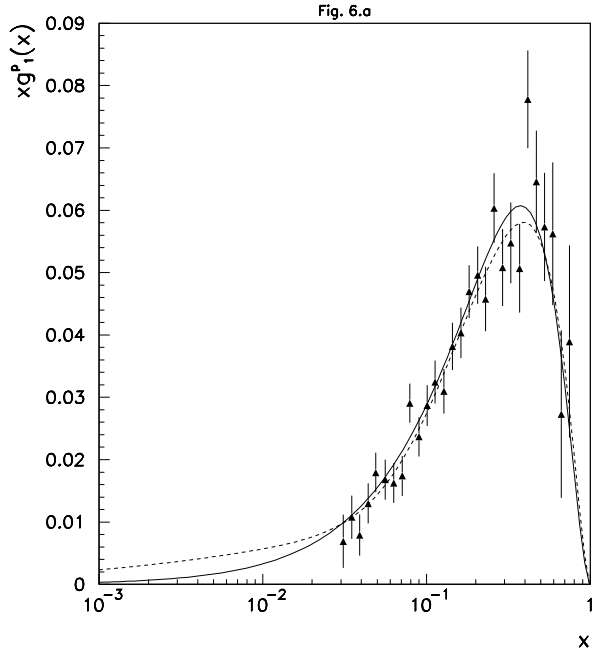


Fig. 6.a The best fit for the options **A** (dashed line) and **B** (solid line) are compared with the SLAC data on proton for $xg_1^p(x)$ at $\langle Q^2 \rangle = 3 \text{ (GeV/c)}^2$ from ref. [11].

Fig. 6.b Same as Fig. 6.a for the deuteron SLAC data for $xg_1^d(x)$ from ref. [11].

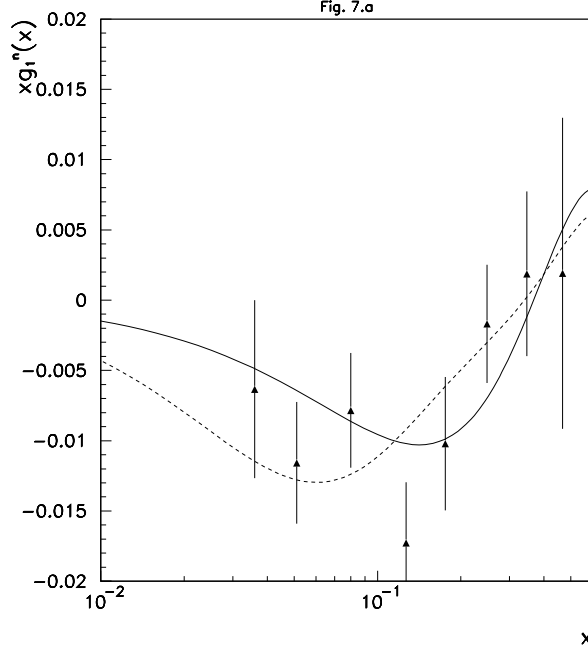


Fig. 7.a The evolution to $Q^2 = 2 (GeV/c)^2$ of the results of the options **A** (dashed line) and **B** (solid line) are compared with the SLAC-E142 data on neutron for $xg_1^n(x)$ at $\langle Q^2 \rangle = 2 (GeV/c)^2$ from ref. [15].

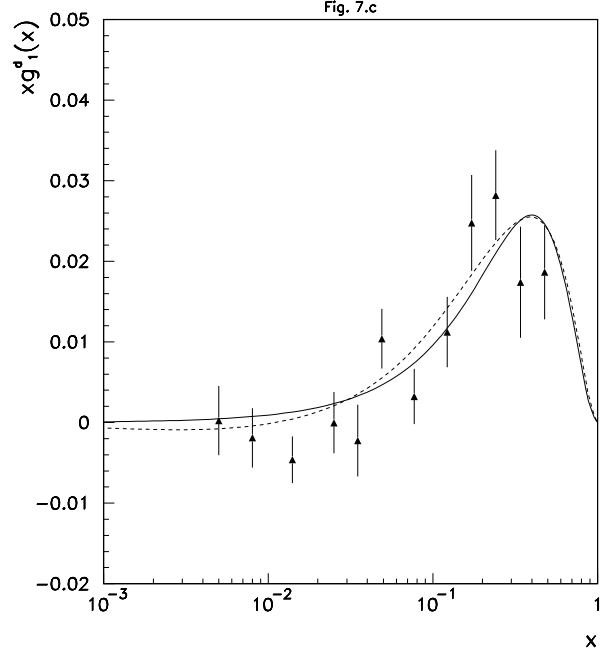
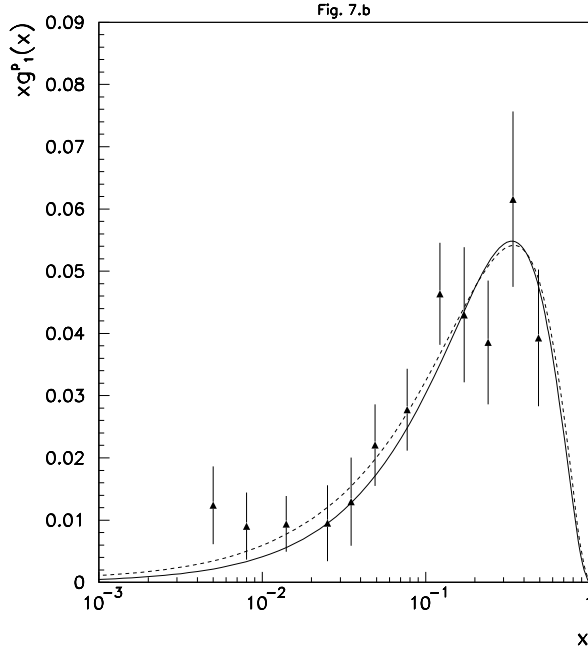


Fig. 7.b The data on proton for $xg_1^p(x)$ from SMC at $\langle Q^2 \rangle = 10 (GeV/c)^2$ from ref. [12] are compared with the results of the options **A** (dashed line) and **B** (solid line), evolved to $Q^2 = 10 (GeV/c)^2$.

Fig. 7.c Same as Fig. 4 for the deuteron SMC data for $xg_1^d(x)$ from ref. [12].